Supplemental Information

Microenvironmental determinants of organized iPSC-cardiomyocyte tissues on synthetic fibrous matrices

Samuel J. DePalma[1], Christopher D. Davidson[1], Austin E. Stis[1], Adam S. Helms[2], Brendon M. Baker[1,+]

[1] Department of Biomedical Engineering, University of Michigan, Ann Arbor, MI 48109

[2]Division of Cardiovascular Medicine, University of Michigan, Ann Arbor, MI 48109

[+] Corresponding Author:

Brendon M. Baker, Ph.D.

Assistant Professor, Department of Biomedical Engineering, University of Michigan

2174 Lurie BME Building, 1101 Beal Avenue

Ann Arbor, MI 48109

Email: bambren@umich.edu

SUPPLEMENTAL FIGURES

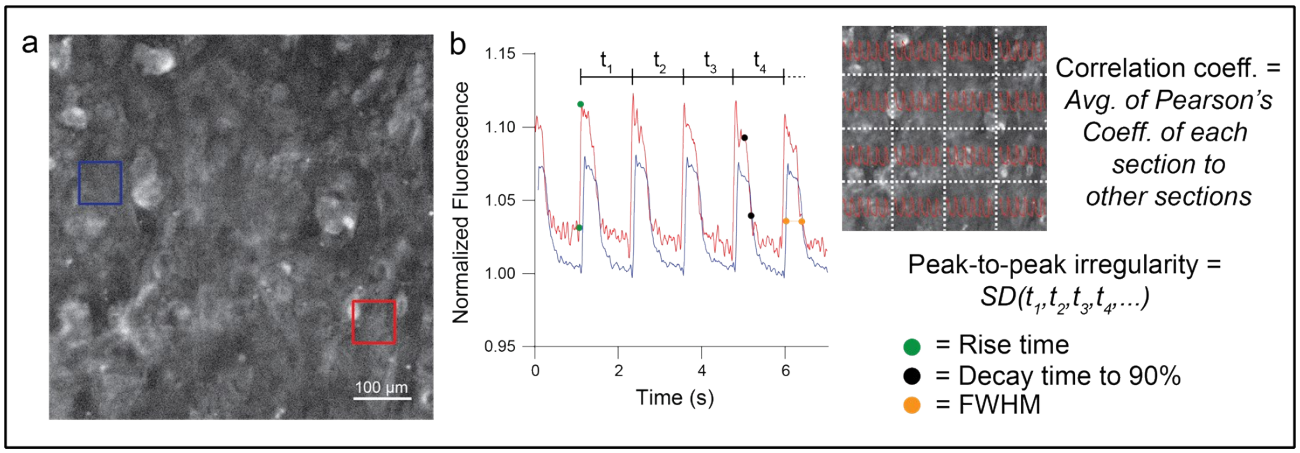

Figure S1: Calcium imaging quantification methodology. Quantification of calcium transients were conducted by capturing time lapse movies at ~100 Hz after the introduction of a calcium sensitive dye. (a) Still frame of sample calcium transient time lapse with two regions indicated that are plotted in (b). (b) Contraction correlation coefficient was determined by calculating the Pearson's correlation coefficient between the flux profiles of multiple regions across the entire tissue. Peak-to-peak irregularity was calculated by finding the standard deviation in the times between subsequent peaks throughout a single time lapse. Flux rise time, decay time, and full width half max are indicated on the flux plots.

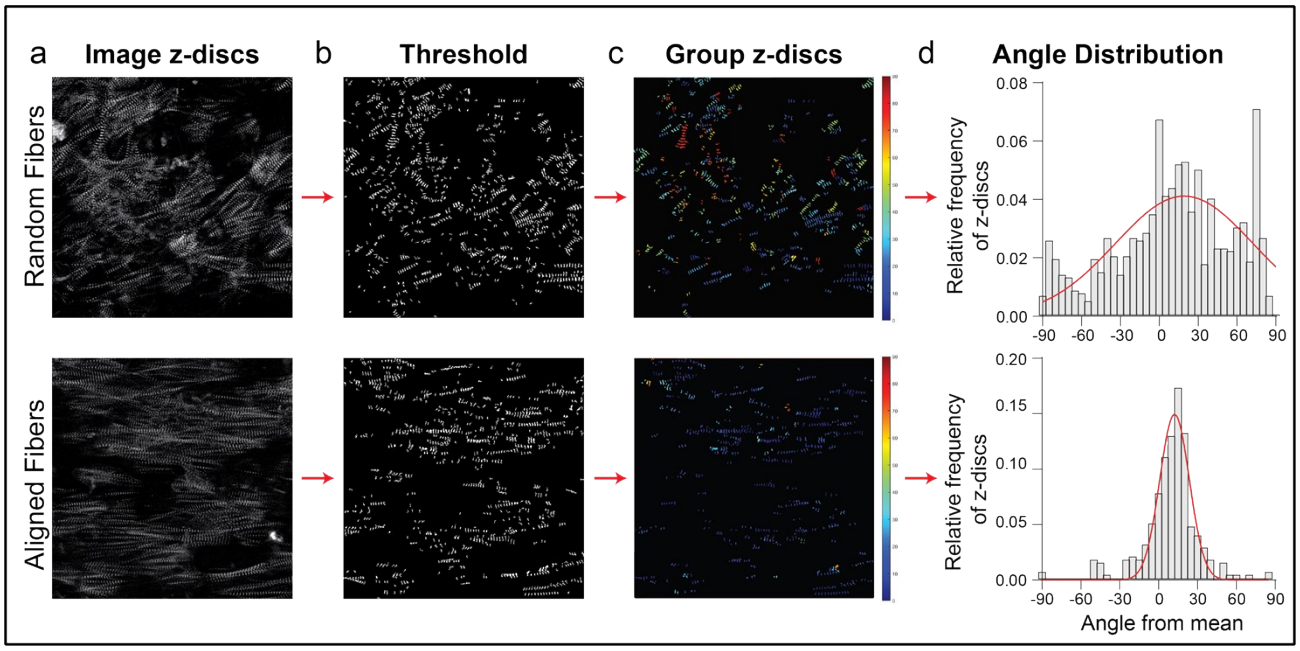

Figure S2: Sarcomere alignment quantification. (a) Myofibril alignment was quantified by processing confocal fluorescent images of titinGFP with a custom Matlab script. (b) Images were thresholded and individual z-discs were identified and (c) grouped based on their orientation and proximity to other z-discs with similar orientation. (d) The distribution of the orientations of groups of z-discs were then plotted and fit to a Gaussian distribution. The standard deviation of this distribution was defined as the sarcomere alignment deviation.

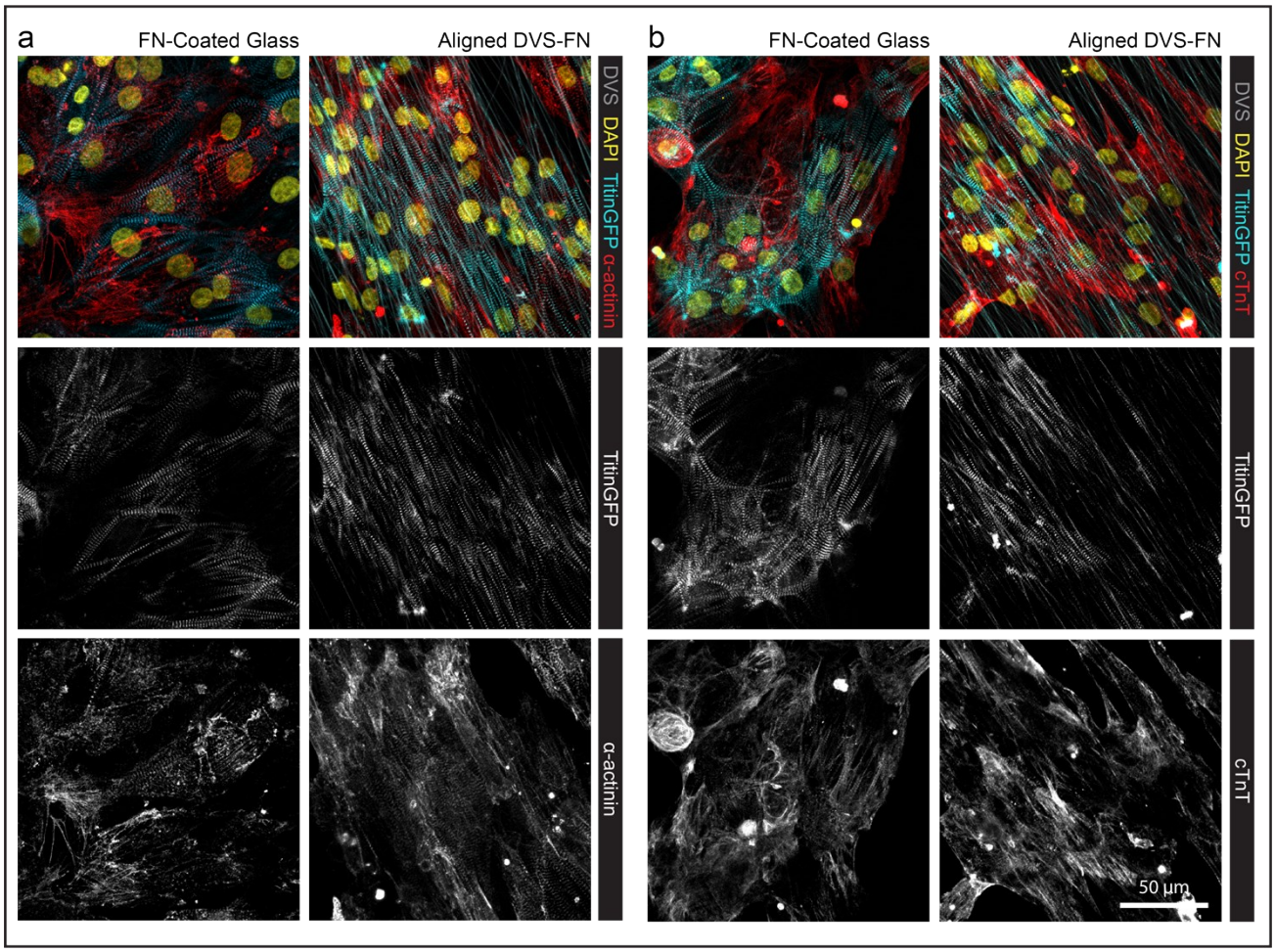

Figure S3: iPSC-CMs express numerous cardiac specific myofibrilar proteins. Confocal fluorescent images of iPSC-CMs containing a titinGFP reporter seeded on FN-coated glass and aligned DVS matrices functionalized with fibronectin stained for (a) α-actinin or (b) cardiac troponin (cTnT).

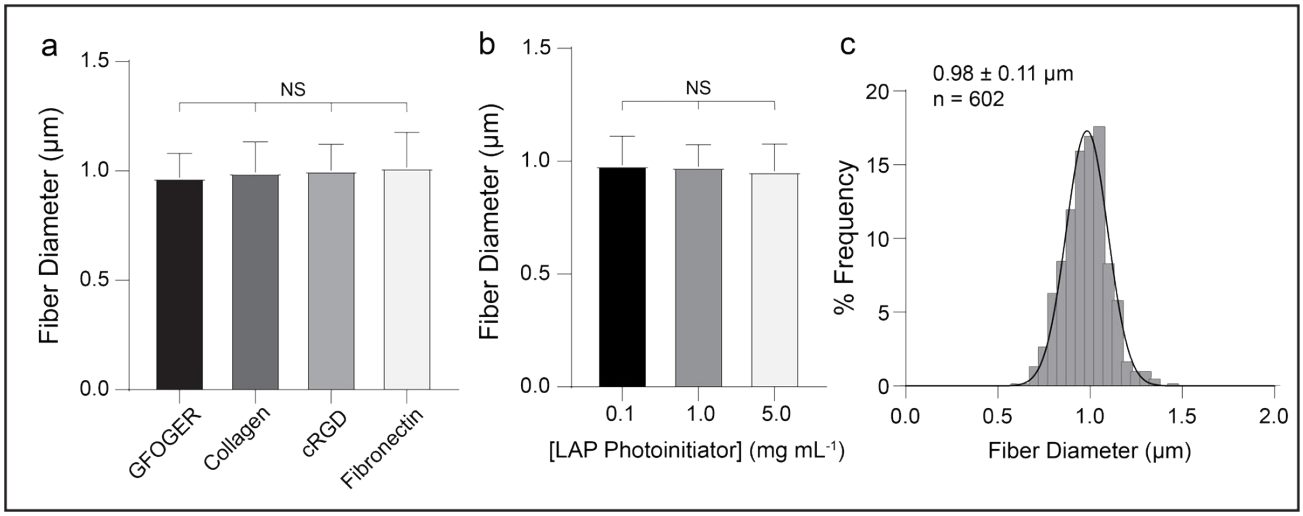

Figure S4: DVS fiber diameter remains constant regardless functionalization scheme or photoinitiated crosslinking. (a) Fiber diameter of DVS fibers crosslinked in 1.0 mg mL^{-1} LAP solution modified with different adhesive moieties. (b) Fiber diameter of DVS fibers crosslinked in the LAP solutions of varied concentration, functionalized with HepMA/FN. All data presented as mean ± std; n ≥ 100 fibers across 10 fields of view; * $p < 0.05$. (c) Histogram of all DVS fiber diameters. Fiber diameters were quantified using ImageJ.

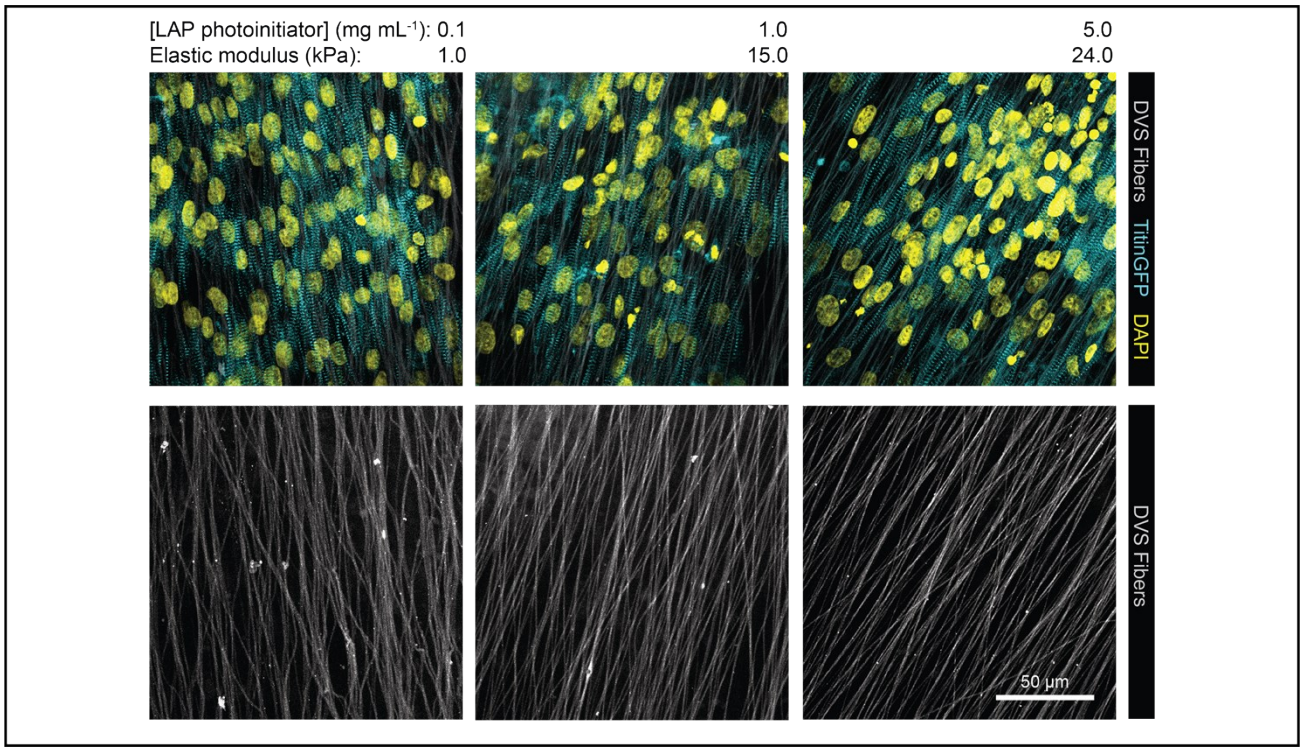

Figure S5: iPSC-CMs deform soft DVS fibers matrices. Confocal fluorescent images of iPSC-CMs cultured on DVS fibers of increasing stiffness. Increased waviness in soft fibers indicate cell-force mediated deformations in soft matrices but not stiffer matrices.

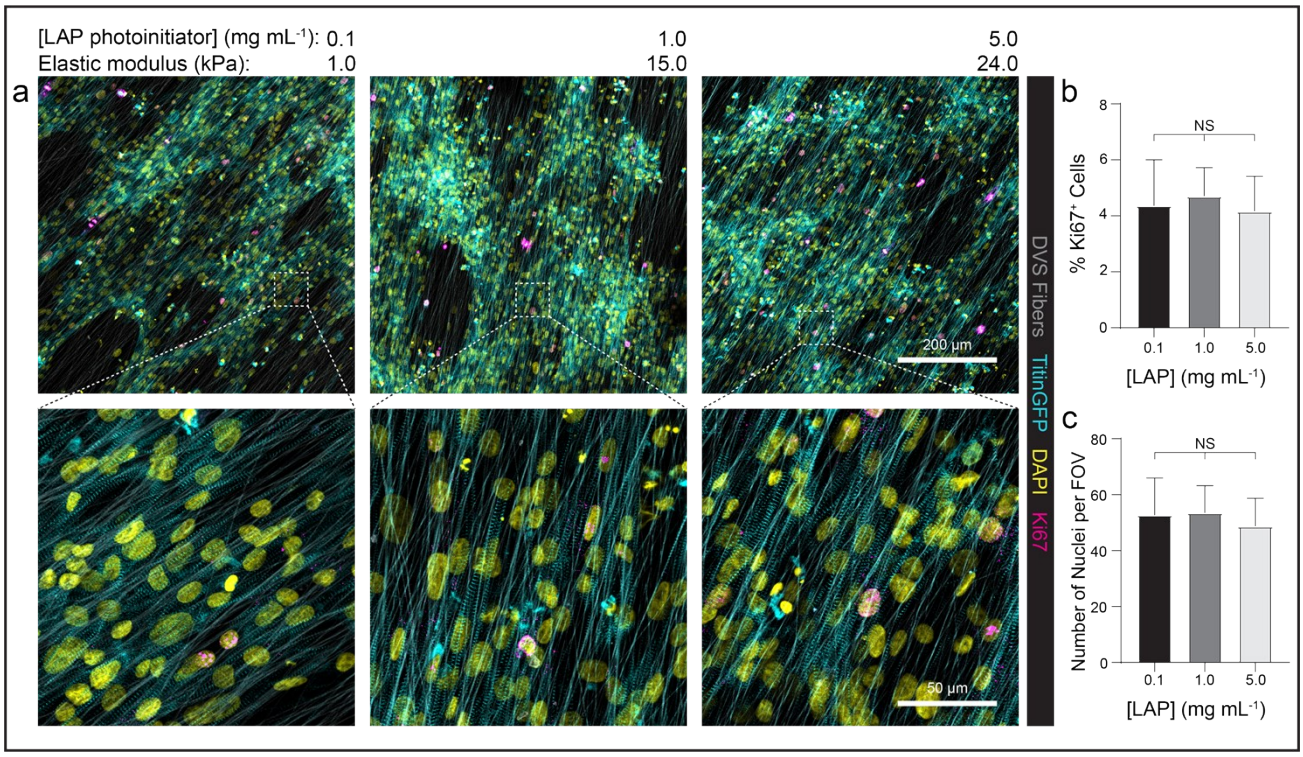

Figure S6: iPSC-CMs remain largely non-proliferative on DVS matrices of different stiffnesses. (a) Confocal fluorescent images at 10x and 40x magnification of iPSC-CMs on aligned matrices composed of DVS fibers of differing stiffness by tuning photoinitiated crosslinking. Immunostaining was performed to visualize Ki67. (b) Quantification of the percentage of total cells expressing nuclear Ki67 across matrices if varied stiffness. (c) Quantification of the number of cells per field of view across matrices of varied stiffness. All data presented as mean ± std; $n \geq 17$ fields of view across 3 tissues; * $p < 0.05$.

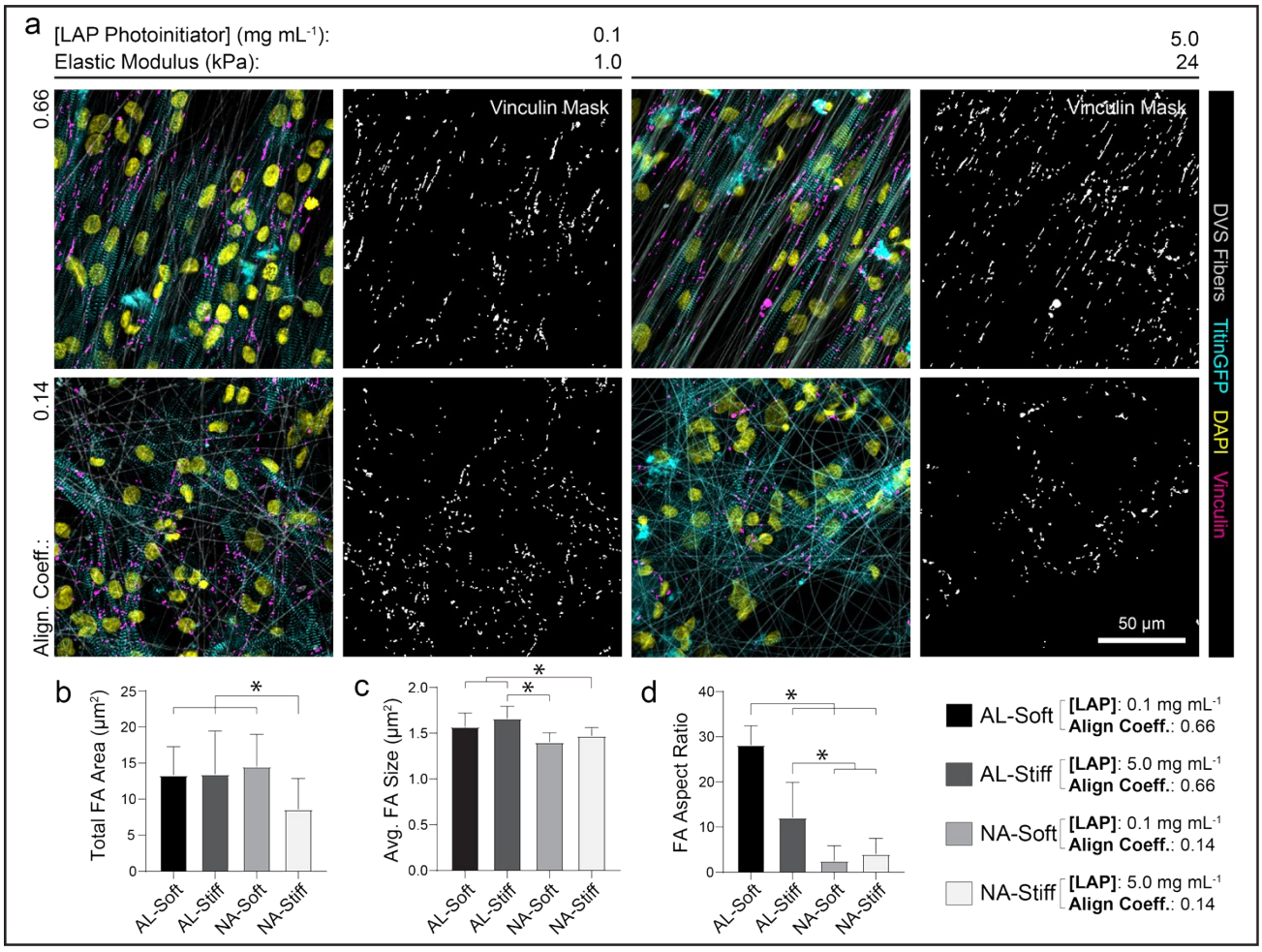

Figure S7: DVS fiber alignment and stiffness synergistically affect iPSC-CM focal adhesion formation. (a) Confocal fluorescent images of iPSC-CMs stained for vinculin on matrices of varied alignment and stiffness. Quantification of (b) total vinculin positive area per cell, (c) average segmented focal adhesion size per cell, (d) and average focal adhesion aspect ratio per cell. All data presented as mean ± std; $n \geq 18$ fields of view across 3 tissues; * $p < 0.05$.

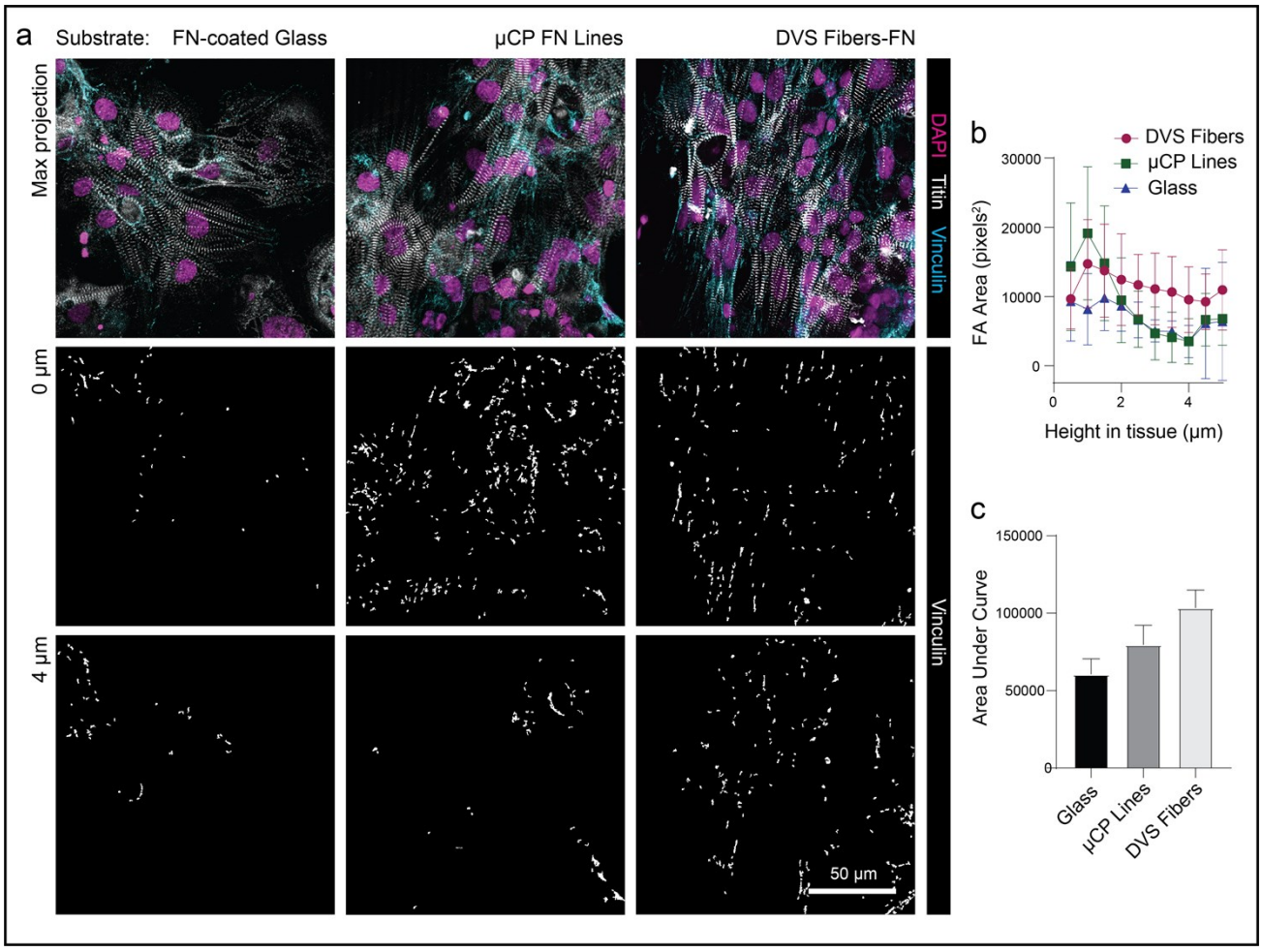

Figure S8: Increased costameres results in more stable culture of iPSC-CMs on DVS fibers. (a) Confocal fluorescent images of iPSC-CMs seeded on fibronectin-coated glass, microcontact printed fibronectin lines, and aligned DexVS fibers modified with adhesive fibronectin. Bottom two rows of images show vinculin at two heights within the tissue. (b) Quantification of vinculin area as a function of height in the tissue. (c) Calculation of area under the curves plotted in (b). All data presented as mean ± std; $n \geq 12$ fibers fields of view; * $p < 0.05$.

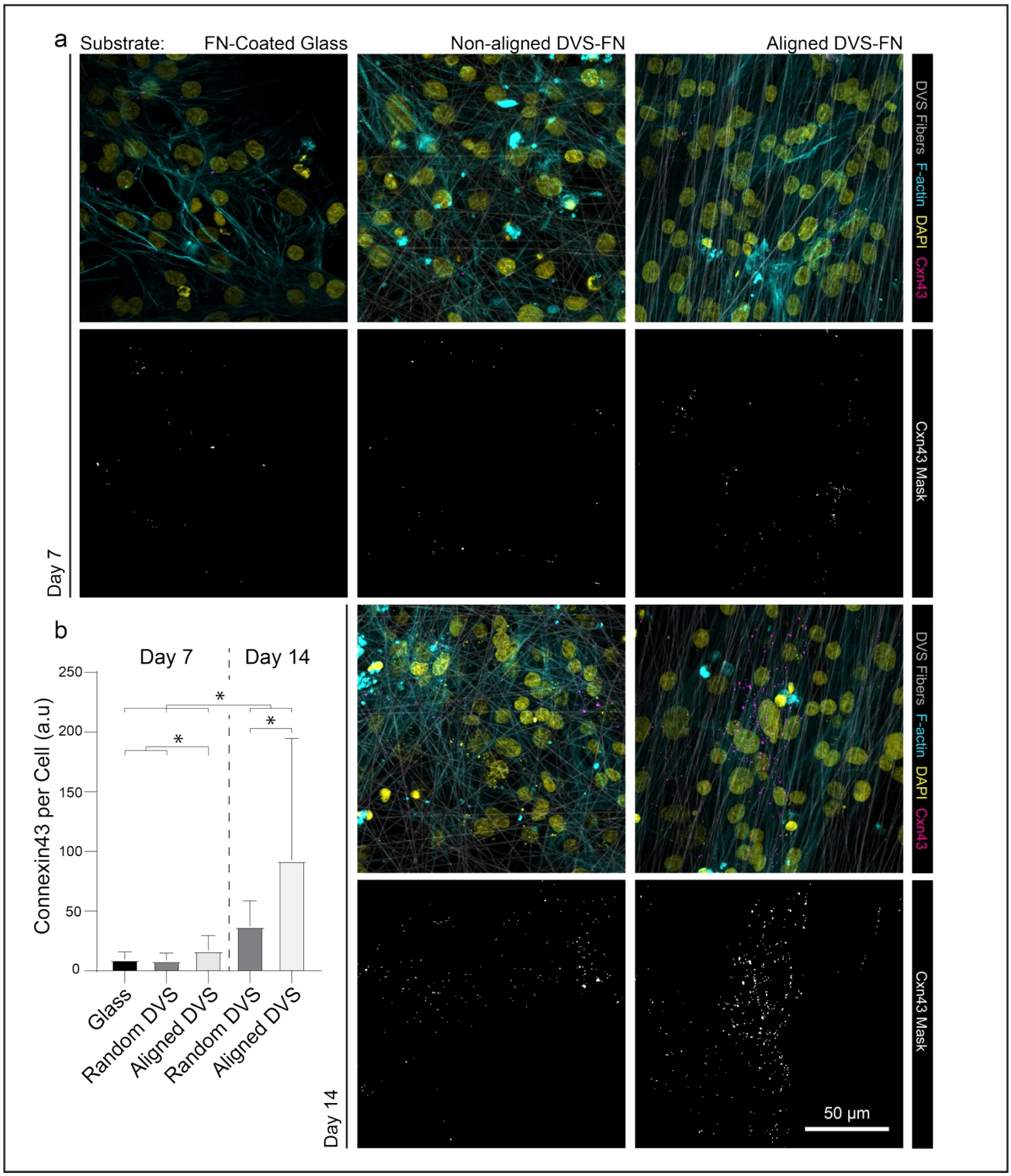

Figure S9: Aligned fibrous matrices enhance iPSC-CM Connexin43 expression. (a) Confocal fluorescent images of iPSC-CM endogenously modified to express connexin43-GFP (Allen Institute; line ID = AICS-0053 cl.16) seeded on FN-coated glass, random DVS matrices, and aligned DVS matrices. Fibrous tissues were imaged on both day 7 and day 14 while iPSC-CMs were imaged only on day 7 due to detachment from the

substrate shortly after this time point. (b) Quantification of connexin43 expression per cell. Data presented as mean ± std; $n \geq 18$ fields of view across 2 tissues; * $p < 0.05$.

SUPPLEMENTAL MOVIES

Movie S1: Calcium transients of iPSC-CMs on DVS matrices presenting varying adhesive moieties.

Movie S2: Calcium transients of iPSC-CMs seeded a varying densities on aligned DVS matrices.

Movie S3: Calcium transients of iPSC-CMs on DVS matrices of varying alignment.

Movie S4: Calcium transients of iPSC-CMs on DVS matrices of varying stiffness.

Movie S5: Calcium transients of iPSC-CMs seeded on FN-coated glass, microcontact printed FN lines, and aligned DVS matrices.